Cardiovascular Revascularization Medicine 68 (2024) 37–42

Contents lists available at ScienceDirect

Cardiovascular Revascularization Medicine

journal homepage: www.sciencedirect.com/journal/cardiovascular-revascularization-medicine

Comparison of interventional treatment options for coronary calcified nodules: A sub-analysis of the ROTA.shock trial

Florian Blachutzik [a,b,*], Sophie Meier [a], Melissa Blachutzik [c], Sophia Schlattner [a,c], Tommaso Gori [d], Helen Ullrich-Daub [d], Luise Gaede [e], Stephan Achenbach [e], Helge Möllmann [f], Bogdan Chitic [f], Adem Aksoy [g], Georg Nickenig [g], Maren Weferling [c], Oliver Dörr [a], Niklas Boeder [a], Matthias Bayer [a], Christian Hamm [a,c], Holger Nef [a,h], on behalf of the ROTA.shock Investigators

[a] Justus Liebig Universität Giessen, Medizinische Klinik 1, Giessen, Germany
[b] Kardiocentrum Frankfurt an der Klinik Rotes Kreuz, Frankfurt am Main, Germany
[c] Kerckhoff-Klinik, Department of Cardiology; German Center for Cardiovascular Research (DZHK), Rhine-Main Partner Site, Bad Nauheim, Germany
[d] Universitätsmedizin Mainz, Kardiologie 1, Mainz, Germany
[e] Universitätsklinikum Erlangen, Medizinische Klinik 2, Erlangen, Germany
[f] St. Johannes-Hospital, Innere Medizin 1, Dortmund, Germany
[g] Universitätsklinikum Bonn, Medizinische Klinik 2, Bonn, Germany
[h] Segeberger Kliniken GmbH, Klinik für Kardiologie und Angiologie, Bad Segeberg, Germany

ARTICLE INFO

Keywords:
Percutaneous coronary intervention
Calcified nodules
Intravascular lithotripsy
Rotational atherectomy
Intravascular imaging

ABSTRACT

Background: The optimal treatment for coronary calcified nodules (CNs) is still unclear. The aim of this study was to compare the modification of these lesions by coronary intravascular lithotripsy (IVL) and rotational atherectomy (RA) using optical coherence tomography (OCT).

Methods: ROTA.shock was a 1:1 randomized, prospective, double-arm multi-center non-inferiority trial that compared the use of IVL and RA with percutaneous coronary intervention (PCI) in severely calcified lesions. In 19 of the patients out of this study CNs were detected by OCT in the target lesion and were treated by either IVL or RA.

Results: The mean angle of CNs was significantly larger in final OCT scans than before RA (92 ± 17° vs. 68 ± 7°; p = 0.01) and IVL (89 ± 18° vs. 60 ± 10°; p = 0.03). The CNs were thinner upon final scans than in initial native scans (RA: 17.8 ± 7.8 mm vs. 38.6 ± 13.1 mm; p = 0.02; IVL: 16.5 ± 9.0 mm vs. 37.2 ± 14.3 mm; p = 0.02). Nodule volume did not differ significantly between native and final OCT scans (RA: 0.66 ± 0.12 mm^3 vs. 0.61 ± 0.33 mm^3; p = 0.68; IVL: 0.64 ± 0.19 mm^3 vs. 0.68 ± 0.22 mm^3; p = 0.74). Final stent eccentricity was high with 0.62 ± 0.10 after RA and 0.61 ± 0.09 after IVL.

Conclusion: RA or IVL are unable to reduce the volume of the calcified plaque. CN modulation seems to be mainly induced by the stent implantation and not by RA or IVL.

1. Introduction

A calcified nodule (CN) is characterized on optical coherence tomography (OCT) scans by intraluminal protrusion of a distinct nodular mass of calcium evolving from an underlying heavily calcified plaque with or without disruption of the intimal fibrous layer [1–6]. According to histology data, >5 % of acute coronary syndromes are caused by thrombosis of CNs [1,5,7,8]. Lee et al. have speculated that CNs may be induced by hinge motion of the vessel, resulting in breaks of calcium sheets and ultimately disruption of the fibrous cap [9,10]. Patients presenting with CNs are usually older and have a high incidence of chronic kidney disease and hypertension [5].

Due to the heavy calcification and the eccentric shape of these intraluminally protruding lesions, interventional treatment of CNs is quite difficult, and current data show unfavorable clinical outcomes after percutaneous coronary intervention (PCI) [11–13]. Therefore, it is imperative to learn more about possible treatment options to improve the clinical outcome of patients with CNs. The aim of this retrospective analysis of data

Abbreviations: CN, Calcified nodule; IVL, Intravascular lithotripsy; LAD, Left anterior descending artery; OCT, Optical coherence tomography; PCI, Percutaneous coronary intervention; RA, Rotational atherectomy; RCA, Right coronary artery.

* Corresponding author at: Kardiocentrum Frankfurt an der Klinik Rotes Kreuz, Königswarterstraße 10, 60316 Frankfurt am Main, Germany.
E-mail address: florian.blachutzik@innere.med.uni-giessen.de (F. Blachutzik).

http://dx.doi.org/10.1016/j.carrev.2024.05.030
Received 15 February 2024; Received in revised form 17 March 2024; Accepted 21 May 2024
Available online 22 May 2024

from the ROTA.shock trial [14] was to analyze and compare the effects of rotational atherectomy (RA) and intravascular lithotripsy (IVL) on CNs as determined by OCT.

2. Material and methods

2.1. Study design and population

This is a retrospective substudy from the ROTA.shock-trial. The ROTA.shock study was a randomized, prospective, double-arm, multi-center non-inferiority trial designed to compare the performance of the Shockwave™ coronary IVL system (Shockwave Medical Inc., Santa Clara, CA, USA) with RA regarding stent dimensions, lumen dimensions, and plaque modulation as determined by OCT as well as regarding procedural success. The primary endpoint was the minimal stent area at the end of the procedure.

From July 2019 until November 2021, 70 patients with clinically significant and severely calcified coronary lesions were included in the ROTA.shock trial in six centers in Germany and were randomly assigned to RA or IVL. The primary inclusion criteria were clinically relevant coronary stenosis with proven myocardial ischemia and severe calcification as defined by coronary angiography: radiopacities noted without cardiac motion before contrast injection and generally compromising both sides of the arterial lumen [15,16]. The primary exclusion criteria were true bifurcation lesions requiring two-stent strategies and cardiogenic shock requiring intravenous catecholamines. Detailed inclusion and exclusion criteria of the ROTA.shock trial have been published previously [14,17]. All patients in whom CNs were detected on OCT in the target lesion were included in the current substudy.

All patients gave their written informed consent before enrollment. The study was conducted in accordance with the Declaration of Helsinki. The study protocol was approved by the ethics committee of the Medical Faculty, Justus-Liebig University Giessen, Giessen, Germany (Number: 231/18). The study was registered at https://www.clinicaltrials.gov with the identifier NCT04047368.

2.2. Study procedure

After randomization to either IVL or RA, PCI was performed via radial or femoral access with a 6 or 7Fr catheter. In a first step, a native OCT of the lesion intended to treat was acquired using a 2.7Fr Dragonfly™ imaging catheter (Optis™, Abbott Vascular, Santa Clara, Ca, USA). The mechanical retraction speed was set to 18 mm/s over a length of 54 mm with automated OCT acquisition. Flushing of the vessel was performed using 20 ml of standard contrast media at an injection rate of 4 ml/s.

If the patient was randomized to RA, a dedicated wire was advanced through the lesion. The burr size was selected according to a burr-to-angiographic reference vessel diameter ratio of 0.5. The rotational speed ranged between 140,000 and 180,000 rotations per minute.

If the patient was randomized to IVL, the IVL balloon catheter (Shockwave C2™, Shockwave Medical Inc., Santa Clara, CA, USA), with diameter selected 1:1 in relation to the angiographic reference vessel diameter, was inserted using a standard coronary guidewire and positioned in the lesion. The balloon was then inflated to 4 atm for each treatment cycle of 10 pulses and subsequently to 6 atm. Treatment cycles were repeated as necessary to cover the whole target lesion, with at least 2–3 cycles being applied to every segment of the calcified lesion.

PCI was continued by non-compliant (NC) balloon dilatation and stent implantation of second-generation drug-eluting stents (e.g. Xience™, Abbott Vascular, Santa Clara, CA, USA) according to current clinical guidelines. The stent diameter was selected according to the angiographically determined reference lumen diameter. After stent implantation, post-dilatation with an NC balloon was obligatory. The NC balloon diameter was either equivalent to the stent diameter or up to 0.5 mm larger.

Upon completion of the procedure, intracoronary nitroglycerine was administered, and a final OCT scan covering the complete stent length was acquired. Dual antiplatelet therapy was prescribed according to current clinical guidelines.

2.3. OCT analysis

OCT image analysis was performed at the core lab (Medizinische Klinik 1, Universitätsklinikum Giessen, Giessen, Germany) using a dedicated OCT analysis software (QIVUS™ OCT Software, Medis, Leiden, Netherlands). OCT cross-sectional images were analyzed at 1-mm intervals using the methods recommended in the expert consensus report for OCT and previous publications [4–6,9]. OCT imaging was carried out before PCI ("native" OCT), after RA or IVL ("post"), and after stent implantation ("final"). To assess the effects of treatment, final OCT scans were analyzed in order to match vessel segments to those in baseline (native) OCT scans using anatomical landmarks (e.g. side branches, characteristic plaque structures). According to previous publications, CNs were identified on OCT as intraluminal protrusions of a distinct nodular mass of calcium evolving from an underlying heavily calcified plaque with or without disruption of the intimal fibrous layer [1–6]. Examples of CNs are displayed in Fig. 1.

2.4. Statistical analysis

Continuous variables are summarized as mean ± standard deviation, and categorical variables are provided as n (%). The Kolmogorov–Smirnov test was performed to test for parametric distribution. To test for statistical differences between two groups for comparison of continuous

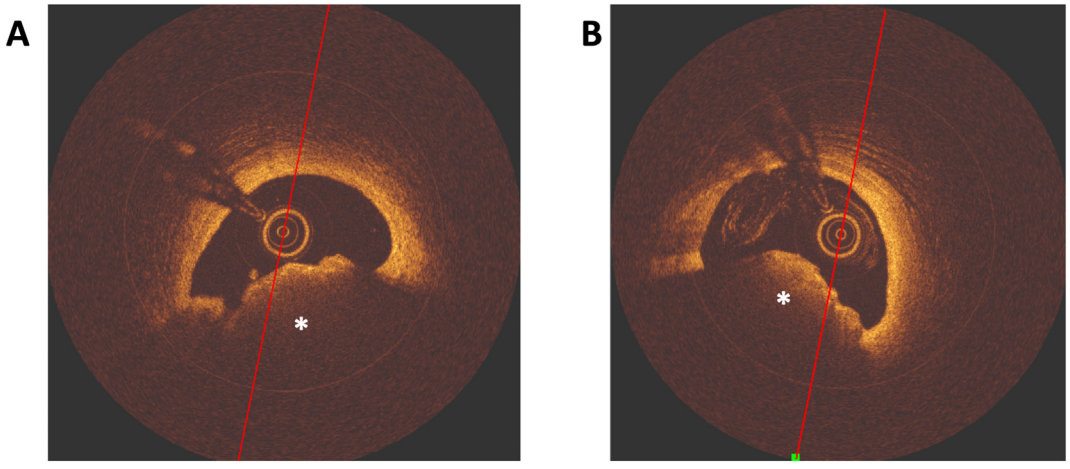

Fig. 1. Two examples for calcified nodules in OCT.
The calcified nodules are marked with asterisks.

variables, either a *t*-test for unpaired samples (parametric distribution) or a Mann–Whitney *U* test (non-parametric distribution) was used. For categorical variables, a Chi-squared or Fisher's exact test was carried out. Statistical analyses were performed using SPSS version 28.0 (IBM SPSS Statistics, IBM Corporation, Armonk, NY, USA). A two-sided $P < 0.05$ was considered significant.

3. Results

3.1. Patient data

A total of 19 patients out of the ROTA.shock main study matched the inclusion criteria for this subanalysis, showing CNs in the treated vessel segment. RA was performed in 7 (37 %) of these patients, IVL in 12 patients (63 %). The mean patient age was 73 ± 9 years and most of the patients were male (15/19; 79 %). There were no significant differences regarding baseline characteristics between the RA and IVL groups (Table 1).

3.2. Procedural data

Most target lesions were located in the left anterior descending artery (LAD) (11/19; 58 %) and in the right coronary artery (RCA) (7/19; 37 %). PCI was performed via radial access in the majority of the patients (14/19; 74 %). Pre-dilatation using NC balloons was performed in 10 out of 19 patients (53 %). The mean IVL balloon diameter was 3.3 ± 0.4 mm, and the mean burr size for RA was 1.5 ± 0.2 mm. Overall, there were no significant differences regarding procedural characteristics between the RA and IVL groups. Additionally, there did not occur any acute complications in the course of PCI in both groups. Detailed procedural data are shown in Table 2.

3.3. Native OCT analysis of calcified nodules

The mean angle of CNs was 63 ± 11°, with a maximum angle of 95 ± 33°. CNs had a mean length of 13.6 ± 11.7 mm, a mean thickness of 37.7 ± 14.0 mm, and a mean volume of 0.66 ± 0.29 mm^3. CNs were associated with an extremely eccentric lumen (maximum lumen eccentricity 0.33 ± 0.12). Plaque erosion of the CNs was present in 8 patients (42 %). Analysis of native OCT scans showed no significant differences in lesion and CN characteristics between the RA and IVL groups. Detailed results are shown in Table 3.

Table 1
Baseline characteristics.

	RA (*n* = 7)	IVL (*n* = 12)	*P*-value
Age (years)	75 ± 7	70 ± 7	0.18
Male	5 (71.4)	10 (83.3)	0.48
BMI (kg/m^2)	28 ± 5	27. ± 5	0.58
Previous MI	2 (28.6)	6 (50.0)	0.12
Previous PCI	4 (57.1)	6 (50.0)	0.72
Previous CABG	2 (28.6)	3 (25.0)	0.66
Hypertension	6 (85.7)	12 (100)	0.45
Diabetes mellitus	3 (42.9)	3 (25.0)	0.3
Hyperlipidemia	3 (42.9)	10 (83.3)	0.12
Active smoking	0 (0)	2 (16.7)	0.21
LVEF (%)	53.9 ± 10.3	55.2 ± 5.0	0.38
Clinical presentation			
STEMI	0 (0)	0 (0)	>0.99
NSTEMI	0 (0)	1 (8.3)	0.45
Unstable angina	0 (0)	1 (8.3)	0.45
Stable CAD	7 (100)	10 (83.3)	0.59

Values are mean ± standard deviation or n (%); Abbreviations: BMI: body-mass index; CABG: coronary artery bypass graft; CAD: coronary artery disease IVL: intravascular lithotripsy; LVEF: left ventricular ejection fraction; MI: myocardial infarction; NSTEMI: non-ST-segment elevated myocardial infarction; PCI: percutaneous coronary intervention; RA: rotational atherectomy; STEMI: ST-segment elevated myocardial infarction.

Table 2
Procedural characteristics.

	RA (n = 7)	IVL (n = 12)	P-value
Target vessel			
LM	0 (0.0)	0 (0.0)	0.72
LAD	4 (57.1)	7 (58.4)	
Cx	0 (0.0)	1 (8.3)	
RCA	3 (42.9)	4 (33.3)	
Femoral access	1 (14.3)	4 (33.3)	0.17
Radial access	6 (85.7)	8 (66.7)	0.43
Max. sheath size (French)	6.2 ± 0.4	6.8 ± 0.6	0.3
Lesion length (mm)	19 ± 7	18 ± 8	0.54
Predilatation	2 (28.6)	8 (66.7)	0.07
Max. pressure (atm)	16.0 ± 3.4	17.0 ± 5.2	0.59
Max. balloon diameter (mm)	3.0 ± 0.7	2.9 ± 0.6	0.92
RA max. burr size (mm)	1.5 ± 0.2		
RA number of runs	2.3 ± 0.9		
IVL balloon diameter (mm)		3.3 ± 0.4	
IVL number of treatment cycles		5.9 ± 2.6	
Stent diameter (mm)	3.6 ± 0.8	3.4 ± 0.4	0.62
Stent length (mm)	26.7 ± 9.7	26.0 ± 8.2	0.87
Postdilatation	7 (100)	12 (100)	>0.99
Max. pressure (atm)	3.7 ± 0.8	20 ± 3	0.75
Max. balloon diameter (mm)	3.8 ± 0.7	19 ± 6	0.77
Contrast media (ml)	162 ± 60	181 ± 66	0.52
Procedure time (min)	63 ± 20	75 ± 21	0.25
Dose-area product ($cGy*cm^2$)	8068 ± 5044	6547 ± 4873	0.8

Values are mean ± standard deviation or n (%); Abbreviations: Cx: circumflex artery; IVL: intravascular lithotripsy; LAD: left anterior descending artery; LM: left main; RA: rotational atherectomy; RCA: right coronary artery.

3.4. Post-RA/IVL OCT analysis of calcified nodules

The mean angle of CNs was 75 ± 23°, with a maximum angle of 114 ± 50°. The mean CN length after RA or IVL was 9.0 ± 5.3 mm, the mean thickness was 29.1 ± 11.0 mm, and the mean volume was 0.63 ± 0.20 mm^3. The maximum lumen eccentricity was 0.38 ± 0.11. Plaque ruptures after RA or IVL were present in 6 patients (32 %), and dissections were present in 9 patients (47 %). The mean lumen gain was 0.42 ± 0.36 mm^2. See Table 4 for detailed results.

3.5. Final OCT analysis of calcified nodules

The mean angle of CNs was 90 ± 18°, and the maximum angle was 140 ± 52°. CNs had a mean length of 12.1 ± 5.3 mm, a mean thickness of 16.9 ± 7.5 mm, and a mean volume of 0.64 ± 0.15 mm^3. The maximum

Table 3
Native OCT analysis of calcified nodules.

	RA (n = 7)	IVL (n = 12)	P-value
Mean angle (°)	68 ± 7	60 ± 10	0.18
Max angle (°)	109 ± 23	86 ± 39	0.31
Mean nodule length (mm)	14.3 ± 7.3	13.3 ± 16.4	0.75
Mean nodule thickness (mm)	38.6 ± 13.1	37.2 ± 14.3	0.89
Mean nodule volume (mm^3)	0.61 ± 0.33	0.68 ± 0.22	0.56
Minimum lumen diameter (mm)	1.82 ± 0.20	2.01 ± 0.51	0.42
Minimum lumen area (mm^2)	2.35 ± 0.76	2.94 ± 1.29	0.47
Maximum lumen diameter (mm)	3.63 ± 0.34	4.26 ± 0.93	0.17
Maximum lumen area (mm^2)	10.40 ± 3.87	14.83 ± 6.71	0.24
Mean lumen diameter (mm)	2.85 ± 0.34	3.05 ± 0.49	0.49
Mean lumen area (mm^2)	6.65 ± 1.57	7.77 ± 2.47	0.41
Maximum lumen eccentricity	0.38 ± 0.07	0.31 ± 0.14	0.31
Mean reference diameter (mm)	2.89 ± 0.55	3.00 ± 0.54	0.62
Plaque rupture	0 (0)	0 (0)	>0.99
Plaque erosion	3 (42.9)	5 (41.7)	0.92
Dissection	0 (0)	0 (0)	>0.99

Values are mean ± standard deviation or n (%); Abbreviations: IVL: intravascular lithotripsy; RA: rotational atherectomy.

Table 4
Post-RA/IVL OCT analysis of calcified nodules.

	RA[a] (n = 7)	IVL (n = 12)	P-value
Mean angle (°)	78 ± 18	73 ± 22	0.63
Max angle (°)	135 ± 60	103 ± 30	0.22
Mean nodule length (mm)	10.4 ± 3.3	8.2 ± 6.7	0.35
Mean nodule thickness (mm)	28.4 ± 9.8	29.5 ± 12.3	0.82
Mean nodule volume (mm^3)	0.63 ± 0.15	0.63 ± 0.26	0.98
Minimum lumen diameter (mm)	2.20 ± 0.28	2.07 ± 0.61	0.55
Minimum lumen area (mm^2)	3.84 ± 0.97	3.64 ± 1.25	0.77
Maximum lumen diameter (mm)	3.85 ± 0.46	3.94 ± 0.75	0.43
Maximum lumen area (mm^2)	11.80 ± 2.72	13.01 ± 4.63	0.74
Mean lumen diameter (mm)	2.97 ± 0.44	3.11 ± 0.49	0.58
Mean lumen area (mm^2)	7.19 ± 2.05	8.14 ± 2.64	0.4
Maximum lumen eccentricity	0.36 ± 0.06	0.38 ± 0.13	0.75
Mean reference diameter (mm)	2.95 ± 0.49	3.09 ± 0.57	0.67
Plaque rupture	4 (57.1)	2 (16.7)	0.19
Dissection	4 (57.1)	5 (41.7)	0.86
Mean lumen gain (mm^2)	0.54 ± 0.48	0.37 ± 0.33	0.32

Values are mean ± standard deviation or n (%); Abbreviations: IVL: intravascular lithotripsy RA: rotational atherectomy.

lumen eccentricity was 0.57 ± 0.09. The mean stent diameter was 3.46 ± 0.53 mm, and the mean stent area was 9.85 ± 3.03 mm^2. The maximum stent eccentricity was 0.61 ± 0.08 (Fig. 2). Stent strut malapposition was present in all 19 patients (100 %). The mean lumen gain was 3.03 ± 2.66 mm^2. Results of the detailed final OCT analysis are shown in Table 5.

Table 5
Final OCT analysis of calcified nodules.

	RA (n = 7)	IVL (n = 12)	P-value
Mean angle (°)	92 ± 17	89 ± 18	0.89
Max angle (°)	145 ± 55	138 ± 47	0.82
Mean nodule length (mm)	13.0 ± 4.9	11.8 ± 5.7	0.55
Mean nodule thickness (mm)	17.8 ± 7.8	16.5 ± 9.0	0.73
Mean nodule volume (mm^3)	0.66 ± 0.12	0.64 ± 0.19	0.94
Minimum lumen diameter (mm)	3.08 ± 0.58	2.91 ± 0.50	0.53
Minimum lumen area (mm^2)	7.68 ± 2.70	6.83 ± 2.29	0.5
Maximum lumen diameter (mm)	4.24 ± 0.77	4.37 ± 0.76	0.72
Maximum lumen area (mm^2)	14.51 ± 4.85	15.44 ± 5.37	0.71
Mean lumen diameter (mm)	3.65 ± 0.65	3.53 ± 0.44	0.68
Mean lumen area (mm^2)	10.81 ± 3.58	10.10 ± 2.51	0.65
Maximum lumen eccentricity	0.60 ± 0.08	0.55 ± 0.08	0.17
Minimum stent diameter (mm)	3.04 ± 0.59	2.80 ± 0.53	0.39
Minimum stent area (mm^2)	7.49 ± 2.74	6.35 ± 2.40	0.38
Maximum stent diameter (mm)	4.10 ± 0.79	4.00 ± 0.56	0.77
Maximum stent area (mm^2)	13.62 ± 4.91	12.78 ± 3.43	0.7
Mean stent diameter (mm)	3.57 ± 0.65	3.41 ± 0.46	0.59
Mean stent area (mm^2)	10.36 ± 3.53	9.42 ± 2.54	0.55
Maximum stent eccentricity	0.62 ± 0.10	0.61 ± 0.09	0.74
Mean reference diameter (mm)	3.10 ± 0.44	3.14 ± 0.50	0.87
Stent expansion	0.82 ± 0.13	0.79 ± 0.13	0.59
Stent malapposition present	7 (100)	12 (100)	>0.99
Maximum distance of malapposition (mm)	0.70 ± 0.14	0.76 ± 0.36	0.65
Mean area of malapposition (mm^2)	0.87 ± 0.61	0.70 ± 0.47	0.53
Mean lumen gain (mm^2)	4.16 ± 2.89	2.33 ± 2.01	0.29

Values are mean ± standard deviation or n (%); Abbreviations: IVL: intravascular lithotripsy RA: rotational atherectomy.

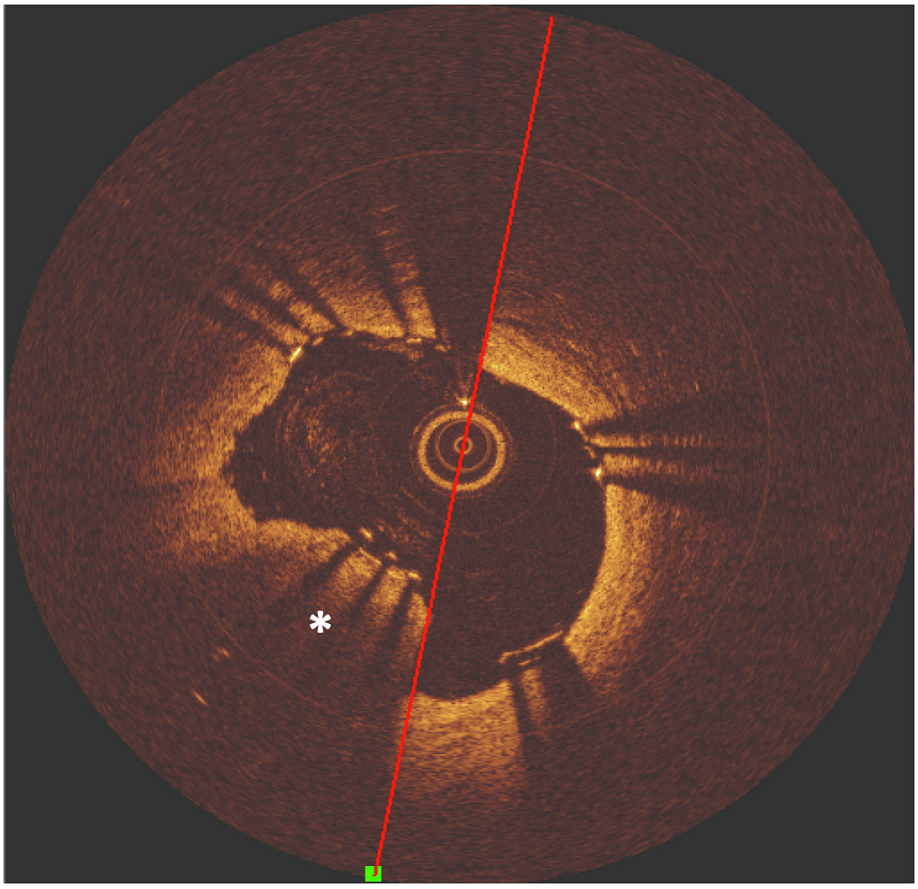

Fig. 2. Eccentric drug-eluting stent after percutaneous coronary intervention of a calcified nodule using intravascular lithoplasty.
The calcified nodule is marked with an asterisk.

3.6. Modulation of calcified nodules by RA

The mean angle of CNs was significantly larger in final OCT scans than in scans made before RA (92 ± 17° vs. 68 ± 7°; $p = 0.01$; Table 6). The mean length of CNs did not differ significantly when comparing final and native OCT images (13.0 ± 4.9 mm vs. 14.3 ± 7.3 mm; $p = 0.67$). The mean thickness of CNs was significantly reduced after RA (17.8 ± 7.8 mm vs. 38.6 ± 13.1 mm; $p = 0.02$). CN volume did not differ significantly (0.66 ± 0.12 mm^3 vs. 0.61 ± 0.33 mm^3; $p = 0.68$; Table 6).

3.7. Modulation of calcified nodules by IVL

The mean angle of CNs was significantly larger after IVL (89 ± 18° vs. 60 ± 10°; $p = 0.03$; Table 7). The mean length of CNs did not differ significantly between final and native OCT scans (11.8 ± 5.7 mm vs. 13.3 ± 16.4 mm; $p = 0.62$). CNs were significantly thinner after IVL (16.5 ± 9.0 mm vs. 37.2 ± 14.3 mm; p = 0.02), although CN volume did not differ significantly (0.64 ± 0.19 mm^3 vs. 0.68 ± 0.22 mm^3; $p = 0.74$; Table 7).

4. Discussion

The main findings of this study are the following: 1) treatment of CNs by RA or IVL does not result in a significant reduction of the plaque mass of the CNs; 2) PCI using RA or IVL leads to a significant reduction in CN thickness; 3) PCI using RA or IVL is associated with a significant increase in the mean angle of CNs; 4) stent eccentricity is high after PCI of CNs using IVL or RA.

To our knowledge this is the first study to analyze the effects of RA and IVL on CNs using OCT. CNs are known to be associated with unfavorable clinical outcomes after implantation of second-generation drug-eluting stents [11,12]. The reasons for this impaired outcome are unclear thus far, but the extensive calcification as well as the eccentricity of the lesions have been discussed as possible causes.

Neither RA nor IVL result in a significant reduction in plaque volume of the CNs. Hence, both techniques fail to promote lumen gain by ablating or compressing the calcified mass of CNs. This may be one important reason for the impaired clinical outcome after PCI of CNs, since inadequate lesion preparation is usually associated with a smaller final lumen area and less-than-optimal stent expansion [6,10,11,18]. Lumen gain seems to be achieved primarily by overexpansion of the vessel.

Significant modifications of CN lesions were only observed after stent implantation, upon final OCT. Both RA and IVL in combination with stent implantation resulted in a significant reduction of CN thickness as well as a significant increase in the mean plaque angle. Hence, CNs are displaced with no significant reduction in their mass. Whether the observed modification of the CNs may occur without prior IVL or RA application, and thus only be an effect of the stent implantation, cannot be clarified based on the data we gathered. It remains unclear whether RA or IVL induce invisible fracturing or "softening" of the CN that improves final stent expansion. However, the clinical data that are available thus far support the hypothesis that PCI of CNs using RA does not lead to an improvement of the result compared to PCI using classical NC-balloon angioplasty prior to stent implantation. Watanabe et al. reported no reduction of the incidence of ischemia-driven target vessel revascularization using RA as compared to NC-balloon dilatation in the interventional treatment of CNs [19].

Stent eccentricity is high after PCI of CNs using RA or IVL (Fig. 2), with no significant differences between the two techniques. Stent eccentricity was 0.62 ± 0.10 after RA and 0.61 ± 0.09 after IVL in this analysis, and a value of <0.7 is usually defined as eccentric [20]. Rheude et al. reported a lower stent eccentricity of 0.70 ± 0.06 after PCI of severely calcified lesions using RA and 0.74 ± 0.09 after using super high-pressure balloons [20]. The high stent eccentricity after PCI of CNs using RA or IVL may contribute to an impaired clinical outcome, since high stent eccentricity is usually associated with higher event rates after PCI [21].

Table 6
Modification of calcified nodules by RA.

	Before RA (n = 7)	Final OCT (n = 7)	P-value
Mean angle (°)	68 ± 7	92 ± 17	0.01
Max angle (°)	109 ± 23	145 ± 55	0.24
Mean nodule length (mm)	14.3 ± 7.3	13.0 ± 4.9	0.67
Mean nodule thickness (mm)	38.6 ± 13.1	17.8 ± 7.8	0.02
Mean nodule volume (mm^3)	0.61 ± 0.33	0.66 ± 0.12	0.68

Values are mean ± standard deviation. Abbreviations: OCT: optical coherence tomography; RA: rotational atherectomy.

Table 7
Modulation of calcified nodules by IVL.

	Before IVL[a] (n = 12)	Final OCT (n = 12)	P-value
Mean angle (°)	60 ± 10	89 ± 18	0.03
Max angle (°)	86 ± 39	138 ± 47	0.06
Mean nodule length (mm)	13.3 ± 16.4	11.8 ± 5.7	0.42
Mean nodule thickness (mm)	37.2 ± 14.3	16.5 ± 9.0	0.02
Mean nodule volume (mm^3)	0.68 ± 0.22	0.64 ± 0.19	0.74

Values are mean ± standard deviation. Abbreviation: IVL: intravascular lithotripsy; OCT: optical coherence tomography.

4.1. Limitations

This study has some important limitations. This is a retrospective analysis with a small number of patients. Despite the fact that ROTA.shock was a randomized clinical trial, this current subanalysis has a selection bias, since only patients in whom CNs were identified in the target lesion in OCT were included. The RA group consisting of 7 patients was smaller than the IVL group, which comprised 12 patients. Nevertheless, there were no significant differences regarding baseline, procedural, and lesions characteristics between the two groups. Therefore, it is unlikely that the different sizes of the groups may have influenced the results.

The reported rate of predilatation may be biased by the fact that the study protocol allowed predilatation in order to acquire a native OCT, and therefore predilatation was sometimes performed just in order to follow the protocol and acquire a native OCT. However, this bias would have affected both groups in the same way and should not have influenced the main result.

Finally, another important limitation is the lack of outcome data, since the aim of this analysis was to evaluate only the acute effects of RA and IVL on CNs.

4.2. Clinical implications

This study is the first to provide morphological explanations for the impaired outcome after PCI in patients with CNs. Both RA and IVL seem to be unable to reduce the plaque volume of CNs, and modification of the nodules, including a reduction in thickness and an increase in the plaque angle, seems to be driven mainly by the stent implantation and not by the previous RA or IVL. Additionally, stent eccentricity remains extremely high after PCI with RA or IVL. Based on the data we gathered, there seems to be no relevant effect of RA or IVL on the CN plaque structure. Whether other techniques such as the use of cutting/scoring balloons, high-pressure balloons, or orbital atherectomy may lead to better results needs to be analyzed in future trials. A combination therapy of RA followed by IVL may also be an alternative for the interventional therapy of CNs, but so far there are only case reports regarding this therapy in severely calcified lesions but not in CNs available. Nevertheless, PCI of CNs will remain challenging due to the high lesion eccentricity and extensive calcification, and it will be important to identify or develop other effective interventional treatment options, since we will encounter these structures more often due to the increasing patient age.

5. Conclusion

PCI with RA and IVL does not lead to a significant reduction of the plaque volume of CNs. CN modification, including a reduction of plaque thickness and an increase in plaque angle, seems to be induced by a displacement of the CNs in the course of stent implantation and not by RA or IVL.

Funding

This study was funded by the Else Kröner-Fresenius-Stiftung, Bad Homburg, Germany. (Grant number: 2019_A17; Grant recipient: Florian Blachutzik).

CRediT authorship contribution statement

Sophie Meier: Writing – review & editing, Validation, Resources, Investigation, Data curation. **Melissa Blachutzik:** Writing – review & editing, Writing – original draft, Visualization, Data curation, Conceptualization. **Sophia Schlattner:** Writing – review & editing, Validation, Data curation, Conceptualization. **Tommaso Gori:** Investigation, Methodology, Writing – review & editing. **Helen Ullrich-Daub:** Data curation, Investigation, Methodology, Resources, Writing – review & editing. **Luise Gaede:** Data curation, Validation, Writing – review & editing. **Stephan Achenbach:** Conceptualization, Investigation, Supervision, Writing – review & editing. **Helge Möllmann:** Data curation, Validation, Writing – review & editing. **Bogdan Chitic:** Data curation, Resources, Writing – review & editing. **Adem Aksoy:** Data curation, Validation, Writing – review & editing. **Georg Nickenig:** Data curation, Validation, Writing – review & editing. **Maren Weferling:** Data curation, Investigation, Writing – review & editing. **Oliver Dörr:** Conceptualization, Investigation, Project administration, Resources, Supervision, Writing – review & editing. **Niklas Boeder:** Data curation, Investigation, Writing – review & editing. **Matthias Bayer:** Data curation, Investigation, Validation, Writing – review & editing. **Christian Hamm:** Conceptualization, Project administration, Supervision, Validation, Writing – review & editing. **Holger Nef:** Conceptualization, Project administration, Supervision, Validation, Writing – review & editing.

Declaration of competing interest

Tommaso Gori received grant support and speaker's honoraria from Abbott vascular and speaker's honoraria from Boston Scientific and Shockwave Medical. Luise Gaede received speaker's honoraria from Abbott vascular, Boston Scientific and Shockwave Medical. Maren Weferling has received speaker's honoraria from Boston Scientific and Shockwave Medical. Helge Möllmann received speaker's honoraria from Boston Scientific and Shockwave Medical. Holger Nef received grant support and speaker's honoraria from Abbott vascular and Shockwave Medical. All other authors report no relevant conflicts of interest.

Acknowledgements

This study was funded by the Else Kröner-Fresenius-Stiftung, Bad Homburg, Germany. (Grant number: 2019_A17; Grant recipient: Florian Blachutzik).

References

[1] Virmani R, Kolodgie FD, Burke AP, Farb A, Schwartz SM. Lessons from sudden coronary death: a comprehensive morphological classification scheme for atherosclerotic lesions. Arterioscler Thromb Vasc Biol. 2000;20(5):1262–75.
[2] Alfonso F, Share Joner M. Untangling the diagnosis and clinical implications of calcified coronary nodules. J Am Coll Cardiol Img. 2017;10(8):892–6.
[3] Jang IK, Tearney GJ, MacNeill B, Takano M, Moselewski F, Iftima N, et al. In vivo characterization of coronary atherosclerotic plaque by use of optical coherence tomography. Circulation. 2005;111:1551–5.
[4] Prati F, Regar E, Mintz GS, Arbustini E, Di Mario C, Jang IK, et al. Expert review document on methodology, terminology, and clinical applications of optical coherence tomography: physical principles, methodology of image acquisition, and clinical application for assessment of coronary arteries and atherosclerosis. Eur Heart J. 2010; 31:401–15.
[5] Jia H, Abtahian F, Aguirre AD, Lee S, Chia S, Lowe H, et al. In vivo diagnosis of plaque erosion and calcified nodule in patients with acute coronary syndrome by intravascular optical coherence tomography. J Am Coll Cardiol. 2013;62:1748–58.
[6] Prati F, Gatto L, Fabbiocchi F, Vergallo R, Paoletti G, Ruscica G, et al. Clinical outcomes of calcified nodules detected by optical coherence tomography: a sub-analysis of the CLIMA study. EuroIntervention. 2020;16(5):380–6.
[7] Naghavi M, Libby P, Falk E, Casscells SW, Litovsky S, Rumberger J, et al. From vulnerable plaque to vulnerable patient: a call for new definitions and risk assessment strategies: part I. Circulation. 2003;108(14):1664–72.
[8] Virmani R, Burke AP, Farb A, Kolodgie FD. Pathology of the vulnerable plaque. J Am Coll Cardiol. 2006;47:C13–8.
[9] Lee T, Mintz GS, Matsumura M, Zhang W, Cao Y, Usui E, et al. Prevalence, predictors, and clinical presentation of a calcified nodule as assessed by optical coherence tomography. J Am Coll Cardiol Img. 2017;10(8):883–91.
[10] Akasaka T, Kubo T. OCT-derived coronary calcified nodules as a predictor of high-risk patients. EuroIntervention. 2020;16(5):361–3.
[11] Morofuji T, Kuramitsu S, Shinozaki T, Jinnouchi H, Sonoda S, Domei T, et al. Clinical impact of calcified nodule in patients with heavily calcified lesions requiring rotational atherectomy. Catheter Cardiovasc Interv. 2021;97(1):10–9.
[12] Madhavan MV, Alsaloum M, Maehara A, Gogia S, Lee J, Fall K, et al. Recurrent calcified nodule protrusion through stent struts after percutaneous coronary intervention of the RCA. J Am Coll Cardiol Intv. 2023;16(19):2463–5.
[13] Sato Y, Finn AV, Virmani R. Calcified nodule: a rare but important cause of acute coronary syndrome with worse clinical outcomes. Atherosclerosis. 2021;318:40–2.
[14] Blachutzik F, Meier S, Weissner M, Schlattner S, Gori T, Ullrich H, et al. Coronary intravascular lithotripsy and rotational atherectomy for severely calcified stenosis: results from the ROTA.shock trial. Catheter Cardiovasc Interv. 2023;102(5):823–33.
[15] Mintz GS, Popma JJ, Pichard AD, Kent KM, Satler LF, Chuang YC, et al. Patterns of calcification in coronary artery disease. A statistical analysis of intravascular ultrasound and coronary angiography in 1155 lesions. Circulation. 1995;91:1959–65.
[16] Abdel-Wahab M, Toelg R, Byrne RA, Geist V, El-Mawardy M, Allali A, et al. High-speed rotational atherectomy versus modified balloons prior to drug-eluting stent implantation in severely calcified coronary lesions. Circ Cardiovasc Interv. 2018;11:e007415.
[17] Blachutzik F, Meier S, Weissner M, Schlattner S, Gori T, Ullrich-Daub H, et al. Comparison of coronary intravascular lithotripsy and rotational atherectomy in the modification of severely calcified stenoses. Am J Cardiol. 2023;197:93–100.
[18] Jinnouchi H, Kuramitsu S, Shinozaki T, Hiromasa T, Kobayashi Y, Takeji Y, et al. Five-year clinical outcomes after drug-eluting stent implantation following rotational atherectomy for heavily calcified lesions. Circ J. 2018;82(4):983–91.
[19] Watanabe Y, Sakakura K, Taniguchi Y, Yamamoto K, Seguchi M, Tsukui T, et al. Comparison of clinical outcomes of intravascular ultrasound-calcified nodule between percutaneous coronary intervention with versus without rotational atherectomy in a propensity-score matched analysis. PloS One. 2020;15(11):e0241836.
[20] Rheude T, Fitzgerald S, Allali A, Mashayekhi K, Gori T, Cuculi F, et al. Rotational atherectomy or balloon-based techniques to prepare severely calcified coronary lesions. J Am Coll Cardiol Intv. 2022;15(18):1864–74.
[21] Suwannasom P, Sotomi Y, Ishibashi Y, Cavalcante R, Albuquerque FN, Macaya C, et al. The impact of post-procedural asymmetry, expansion, and eccentricity of bioresorbable everolimus-eluting scaffold and metallic everolimus-eluting stent on clinical outcomes in the ABSORB II trial. J Am Coll Cardiol Intv. 2016;9(12):1231–42.